

## Polymer Brushes on Single-Walled Carbon Nanotubes by Atom Transfer Radical Polymerization of *n*-Butyl Methacrylate

Shuhui Qin,<sup>†</sup> Dongqi Qin,<sup>†</sup> Warren T. Ford,<sup>\*,†</sup> Daniel E. Resasco,<sup>‡</sup> and Jose E. Herrera<sup>‡</sup>

Contribution from the Department of Chemistry, Oklahoma State University, Stillwater, Oklahoma 74078, and School of Chemical and Materials Engineering, University of Oklahoma, Norman, Oklahoma 73019

Received August 14, 2003; E-mail: wtford@okstate.edu

**Abstract:** Polymer brushes with single-walled carbon nanotubes (SWNT) as backbones were synthesized by grafting *n*-butyl methacrylate (nBMA) from the ends and sidewalls of SWNT via atom transfer radical polymerization (ATRP). Carboxylic acid groups on SWNT were formed by nitric acid oxidation. The ATRP initiators were covalently attached to the SWNT by esterification of 2-hydroxyethyl 2'-bromopropionate with carboxylic acid groups. Methyl 2-bromopropionate (MBP) was added as free initiator during the brush preparation to control growth of the brushes and to monitor the polymerization kinetics. Size-exclusion chromatography (SEC) results show that the molecular weight of free poly(*n*-butyl methacrylate) (PnBMA) increased linearly with nBMA monomer conversion. PnBMA cleaved from the SWNT after high conversion had the same molecular weight as PnBMA produced in solution. Thermogravimetric analyses (TGA) show that the amount of PnBMA grown from the SWNT increased linearly with the molecular weight of the free PnBMA. The most highly PnBMA-functionalized SWNT dissolve in 1,2-dichlorobenzene, chloroform, and tetrahydrofuran, and solubility increases with the amount of PnBMA bound to SWNT. Near-infrared and Raman spectra indicate that the side walls of the SWNT were lightly functionalized by the nitric acid treatment and that the degree of functionalization of the SWNT did not change significantly during the formation of initiator or during the polymerization. Atomic force microscopy (AFM) images show contour lengths of the SWNT brushes on a mica surface from 200 nm to 2.0  $\mu\text{m}$  and an average height of the backbone of 2–3 nm, indicating that the bundles of original SWNT were broken into individual tubes by functionalization and polymerization.

### Introduction

Single-walled carbon nanotubes (SWNT) are leading to the development of new nanotechnologies because of their outstanding electronic, mechanical, and thermal properties.<sup>1–4</sup> SWNT have the greatest tensile modulus and tensile strength of any known materials. Composites of SWNT and poly(vinyl alcohol) are the strongest known so far.<sup>5</sup> By blending SWNT in small amounts in the form of small bundles or individual tubes, they should markedly increase the mechanical strength, the electrical conductivity, and the thermal conductivity of other polymers.<sup>6,7</sup> However, there is no general solution to dispersion of SWNT in polymers. Their insolubility in solvents due to strong intertube van der Waals attraction impedes their applica-

tion.<sup>8</sup> Noncovalent or covalent functionalization improves the solubility. Noncovalent functionalization methods include dispersion with low molar mass or block copolymer surfactants,<sup>9–11</sup> polymer wrapping,<sup>12–14</sup> and polymer absorption<sup>15,16</sup> in which the polymers are produced by in situ ring opening metathesis polymerization or emulsion polymerization. The advantage of noncovalent attachment is that the nanotube structure and its electronic properties are not altered, but the surfactants and polymers that can be used for this method are limited. Covalent

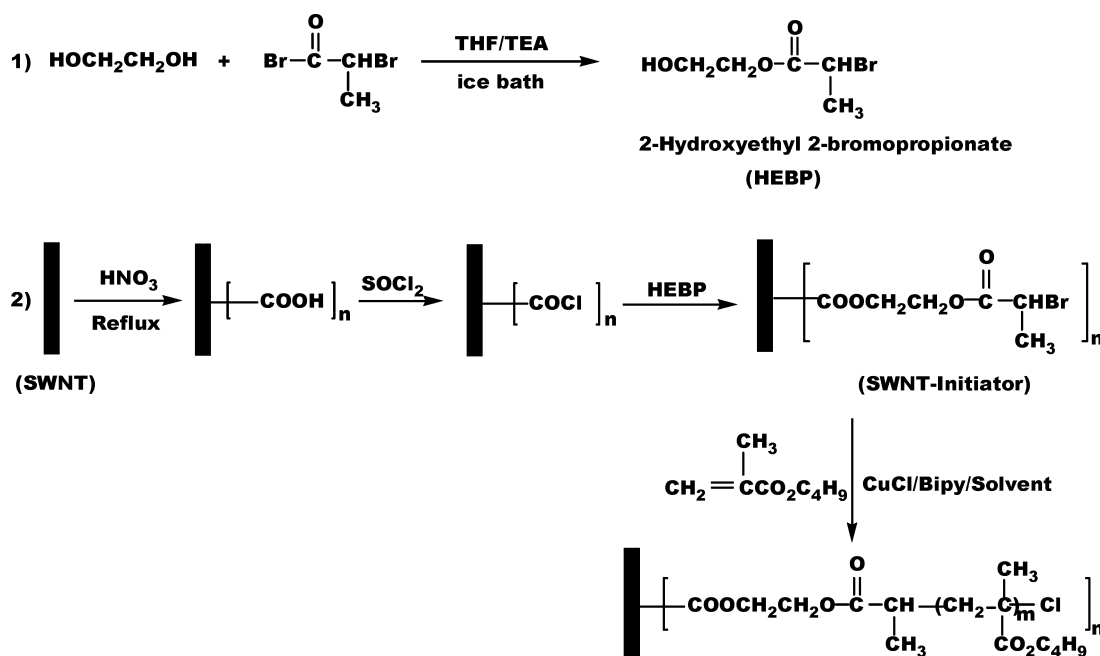
<sup>†</sup> Oklahoma State University.

<sup>‡</sup> University of Oklahoma.

- (1) Dresselhaus, M. S.; Dresselhaus, G.; Eklund, P. C., Eds. *Science of Fullerenes and Carbon Nanotubes*; 1996.
- (2) Ajayan, P. M. *Chem. Rev.* **1999**, *99*, 1787–1799.
- (3) Dai, H. *Acc. Chem. Res.* **2002**, *35*, 1035–1044.
- (4) Hirsch, A. *Angew. Chem., Int. Ed.* **2002**, *41*, 1853–1859.
- (5) Dalton, A. B.; Collins, S.; Munoz, E.; Razal, J. M.; Ebron, V. H.; Ferraris, J. P.; Coleman, J. N.; Kim, B. G.; Baughman, R. H. *Nature* **2003**, *423*, 703.
- (6) Ajayan, P. M.; Schadler, L. S.; Giannaris, C.; Rubio, A. *Adv. Mater.* **2000**, *12*, 750–753.
- (7) Kearns, J. C.; Shambaugh, R. L. *J. Appl. Polym. Sci.* **2002**, *86*, 2079–2084.

- (8) Baughman, R. H.; Zakhidov, A. A.; de Heer, W. A. *Science* **2002**, *297*, 787–792.
- (9) Islam, M. F.; Rojas, E.; Bergey, D. M.; Johnson, A. T.; Yodh, A. G. *Nano Lett.* **2003**, *3*, 269–273.
- (10) O'Connell, M. J.; Bachilo, S. M.; Huffman, C. B.; Moore, V. C.; Strano, M. S.; Haroz, E. H.; Rialon, K. L.; Boul, P. J.; Noon, W. H.; Kittrell, C.; Ma, J.; Hauge, R. H.; Weisman, R. B.; Smalley, R. E. *Science* **2002**, *297*, 593–596.
- (11) Kang, Y.; Taton, T. A. *J. Am. Chem. Soc.* **2003**, *125*, 5650–5651.
- (12) O'Connell, M. J.; Boul, P.; Ericson, L. M.; Huffman, C.; Wang, Y.; Haroz, E.; Kuper, C.; Tour, J.; Ausman, K. D.; Smalley, R. E. *Chem. Phys. Lett.* **2001**, *342*, 265–271.
- (13) Star, A.; Stoddart, J. F.; Steuerman, D.; Diehl, M.; Boukai, A.; Wong, E. W.; Yang, X.; Chung, S.-W.; Choi, H.; Heath, J. R. *Angew. Chem., Int. Ed.* **2001**, *40*, 1721–1725.
- (14) Star, A.; Steuerman, D. W.; Heath, J. R.; Stoddart, J. F. *Angew. Chem., Int. Ed.* **2002**, *41*, 2508–2512.
- (15) Gomez, F. J.; Chen, R. J.; Wang, D.; Waymouth, R. M.; Dai, H. *Chem. Commun.* **2003**, 190–191.
- (16) Barraza, H. J.; Pompeo, F.; O'Rear, E. A.; Resasco, D. E. *Nano Lett.* **2002**, *2*, 797–802.

Scheme 1



functionalization can be realized by either modification of carboxylic acid groups on the SWNT or direct addition of reagents to the sidewalls of SWNT. Carboxylic acid groups are introduced at the sidewalls and open ends of SWNT by nitric acid oxidation, and long alkyl chains, polymers, and sugars have been attached by esterification or amidation reactions.<sup>17–21</sup> Living anionic polymerization of styrene from SWNT has been used to produce a composite containing less than 20 wt % polystyrene.<sup>22</sup> Species added to the sidewalls include fluorine,<sup>23</sup> aryl radicals,<sup>24</sup> aryl cations,<sup>25</sup> hydrogen,<sup>26</sup> nitrenes,<sup>27</sup> carbenes,<sup>27,28</sup> radicals,<sup>4,29</sup> and 1,3-dipoles.<sup>30</sup> Most direct addition approaches lead to soluble materials. The control of functionalization density is difficult, and high functionalization density is necessary for high solubility because the attached organic molecules are very small compared with the tube length. For example, the degree of functionalization is 1 in 2 carbons in fluorination,<sup>23</sup> 1 in 5 carbons in radical addition,<sup>29</sup> and 1 in 8–12 carbons in replacement of fluorine by terminal diamines.<sup>31</sup> However, the electronic and spectroscopic properties of SWNT

are altered by conversion of sidewall carbon atoms from trigonal to tetrahedral bonding.

A solution for higher solubility of SWNT with little loss of the electronic properties is functionalization by polymers. Here we report the first preparation of polymer brushes from the SWNT by functionalizing the ends and sidewalls of the tube with ATRP initiators and subsequent grafting of poly(*n*-butyl methacrylate) (PnBMA) as shown in Scheme 1.

A polymer brush is an assembly of polymer chains that are tethered by one end to a substrate,<sup>32,33</sup> such as a silicon wafer,<sup>33–37</sup> gold, latex, and carbon black particles,<sup>33,38–40</sup> and long polymer backbones.<sup>41–43</sup> Polymer brushes have recently attracted considerable attention because of their novel structures and properties.<sup>33,44,45</sup> Polymer brushes were first synthesized by physisorption of block copolymers onto a substrate, with one block adsorbing strongly to the substrate surface and the other block forming the brush layer.<sup>46</sup> However, thermal and solvolytic

- (17) Chen, J.; Hamon, M. A.; Hu, H.; Chen, Y.; Rao, A. M.; Eklund, P. C.; Haddon, R. C. *Science* **1998**, *282*, 95–98.  
 (18) Sun, Y.-P.; Fu, K.; Lin, Y.; Huang, W. *Acc. Chem. Res.* **2002**, *35*, 1096–1104.  
 (19) Sano, M.; Kamino, A.; Okamura, J.; Shinkai, S. *Langmuir* **2001**, *17*, 5125–5128.  
 (20) Niyogi, S.; Hamon, M. A.; Hu, H.; Zhao, B.; Bhowmik, P.; Sen, R.; Itkis, M. E.; Haddon, R. C. *Acc. Chem. Res.* **2002**, *35*, 1105–1113.  
 (21) Pompeo, F.; Resasco, D. E. *Nano Lett.* **2002**, *2*, 369–373.  
 (22) Viswanathan, G.; Chakrapani, N.; Yang, H.; Wei, B.; Chung, H.; Cho, K.; Ryu, C. Y.; Ajayan, P. M. *J. Am. Chem. Soc.* **2003**, *125*, 9258–9259.  
 (23) Mickelson, E. T.; Huffman, C. B.; Rinzler, A. G.; Smalley, R. E.; Hauge, R. H.; Margrave, J. L. *Chem. Phys. Lett.* **1998**, *296*, 188–194.  
 (24) Bahr, J. L.; Yang, J.; Kosynkin, D. V.; Bronikowski, M. J.; Smalley, R. E.; Tour, J. M. *J. Am. Chem. Soc.* **2001**, *123*, 6536–6542.  
 (25) Dyke, C. A.; Tour, J. M. *J. Am. Chem. Soc.* **2003**, *125*, 1156–1157.  
 (26) Pekker, S.; Salvetat, J. P.; Jakab, E.; Bonard, J. M.; Forro, L. *J. Phys. Chem. B* **2001**, *105*, 7938–7943.  
 (27) Holzinger, M.; Vostrowsky, O.; Hirsch, A.; Hennrich, F.; Kappes, M.; Weiss, R.; Jellen, F. *Angew. Chem., Int. Ed.* **2001**, *40*, 4002–4005.  
 (28) Chen, Y.; Haddon, R. C.; Fang, S.; Rao, A. M.; Eklund, P. C.; Lee, W. H.; Dickey, E. C.; Grulke, E. A.; Pendergrass, J. C.; Chavan, A.; Haley, B. E.; Smalley, R. E. *J. Mater. Res.* **1998**, *13*, 2423–2431.  
 (29) Ying, Y.; Saini, R. K.; Liang, F.; Sadana, A. K.; Billups, W. E. *Org. Lett.* **2003**, *5*, 1471–1473.  
 (30) Georgakilas, V.; Kordatos, K.; Prato, M.; Guldi, D. M.; Holzinger, M.; Hirsch, A. *J. Am. Chem. Soc.* **2002**, *124*, 760–761.

- (31) Stevens, J. L.; Huang, A. Y.; Peng, H.; Chiang, I. W.; Khabashesku, V. N.; Margrave, J. L. *Nano Lett.* **2003**, *3*, 331–336.  
 (32) Milner, S. T. *Science* **1991**, *251*, 905–914.  
 (33) Zhao, B.; Brittain, W. J. *Prog. Polym. Sci.* **2000**, *25*, 677–710.  
 (34) Huang, W.; Skanth, G.; Baker, G. L.; Bruening, M. L. *Langmuir* **2001**, *17*, 1731–1736.  
 (35) Matyjaszewski, K.; Miller, P. J.; Shukla, N.; Immaraporn, B.; Gelman, A.; Luokala, B. B.; Siclován, T. M.; Kickelbick, G.; Vallant, T.; Hoffmann, H.; Pakula, T. *Macromolecules* **1999**, *32*, 8716–8724.  
 (36) Husseman, M.; Malmstroem, E. E.; McNamara, M.; Mate, M.; Mecerreyes, D.; Benoit, D. G.; Hedrick, J. L.; Mansky, P.; Huang, E.; Russell, T. P.; Hawker, C. J. *Macromolecules* **1999**, *32*, 1424–1431.  
 (37) Ejaz, M.; Yamamoto, S.; Ohno, K.; Tsujii, Y.; Fukuda, T. *Macromolecules* **1998**, *31*, 5934–5936.  
 (38) Ohno, K.; Koh, K.-m.; Tsujii, Y.; Fukuda, T. *Macromolecules* **2002**, *35*, 8989–8993.  
 (39) Vestal, C. R.; Zhang, Z. J. *J. Am. Chem. Soc.* **2002**, *124*, 14312–14313.  
 (40) Liu, T.; Jia, S.; Kowalewski, T.; Matyjaszewski, K.; Casado-Portilla, R.; Belmont, J. *Langmuir* **2003**, *19*, 6342–6345.  
 (41) Beers, K. L.; Gaynor, S. G.; Matyjaszewski, K.; Sheiko, S. S.; Moeller, M. *Macromolecules* **1998**, *31*, 9413–9415.  
 (42) Boerner, H. G.; Beers, K.; Matyjaszewski, K.; Sheiko, S. S.; Moeller, M. *Macromolecules* **2001**, *34*, 4375–4383.  
 (43) Matyjaszewski, K.; Qin, S.; Boyce, J. R.; Shirvanyants, D.; Sheiko, S. S. *Macromolecules* **2003**, *36*, 1843–1849.  
 (44) Ito, Y.; Nishi, S.; Park, Y. S.; Imanishi, Y. *Macromolecules* **1997**, *30*, 5856–5859.  
 (45) Mayes, A. M.; Kumar, S. K. *MRS Bull.* **1997**, *22*, 43–47.  
 (46) Hadziioannou, G.; Patel, S.; Granick, S.; Tirrell, M. *J. Am. Chem. Soc.* **1986**, *108*, 2869–2876.

desorption of the brush due to the weak noncovalent nature of the grafting and a limited choice of functional groups for block copolymer synthesis are two major disadvantages to this strategy. Covalent attachment of polymer chains to the surface can be accomplished by either "grafting to" or "grafting from" techniques. "Grafting to" involves the bonding of a preformed end-functionalized polymer to reactive surface groups on the substrate.<sup>47</sup> The limitation in this technique is that attachment of a small number of chains hinders diffusion of additional macromolecules to the surface, thereby leading to low grafting density. The "grafting from" technique involves the immobilizing of initiators onto the substrate followed by in situ surface-initiated polymerization to generate the tethered polymer chains.<sup>33</sup> Initiators can be immobilized onto the substrate surfaces by treatment of a substrate with glow discharge or plasma in the presence of a gas<sup>48</sup> or by chemical methods.<sup>35–37,39,41</sup> The advantage of this technique is that polymer brushes with high grafting density are easily synthesized. For better control of molecular weight and molecular weight distribution of the tethered polymers and to form block copolymer brushes, living radical, anionic, carbocationic, and ring-opening metathesis polymerizations have been used in "grafting from" methods.<sup>33,35–37,39,41,49–51</sup> Living radical polymerization, especially atom transfer radical polymerization (ATRP),<sup>52</sup> is the method used most to graft polymer chains of controlled molecular weight from silicon wafers, gold particles, and polymer backbones.

## Experimental Section

**Materials.** *n*-Butyl methacrylate (Fluka,  $\geq 99\%$ ) was purified by passage through basic alumina and vacuum distillation. Thionyl chloride ( $\text{SOCl}_2$ , Aldrich, 99+%), ethylene glycol (Acros, 97%), 2-bromopropionyl bromide (Aldrich, 97%), methyl 2-bromopropionate (MBP) (Aldrich, 98%), 2,2'-bipyridine (bipy) (Aldrich, 99+%), and CuCl (Aldrich, 99.995+%) were used as received. Triethylamine (TEA) was dried over anhydrous  $\text{MgSO}_4$ . 1,2-Dichlorobenzene (DCB) and other solvents were used as received from Aldrich or Acros Chemicals. Single-walled carbon nanotubes were purchased from Carbon Nanotechnologies Inc., Houston, TX (HiPco, batch CM260015-6) and functionalized with carboxylic acid groups by oxidation with 2.6 M nitric acid.<sup>53</sup>

**Instruments and Measurements.** Monomer conversion was determined from 300 MHz  $^1\text{H}$  NMR spectra by use of DCB as internal standard. Elemental analyses were done at Midwest Microlab, Indianapolis, IN. Molecular weights were measured by size-exclusion chromatography (SEC) on an Agilent series 1100 chromatograph with tetrahydrofuran (THF) as eluent (1 mL/min) at 40 °C with differential refractive index detection, and two Polymer Laboratories columns (PL gel 10  $\mu\text{m}$  mixed B, 7.5 mm ID). Polystyrene standards in the range of 1 800 000–500 g/mol were used for specific calibration. TGA data were obtained in a nitrogen atmosphere with a Shimadzu TGA50/50H thermogravimetric analyzer. Raman spectra were recorded on a Jovin Yvon-Horiba Lab Raman spectrometer equipped with a charge-coupled

device (CCD) detector and 633 nm laser excitation.<sup>54</sup> Near-IR and mid-IR spectra were recorded on Bruker Equinox 55 Fourier transform infrared/near-infrared (FTIR/FTNIR) and Perkin-Elmer 2000 FTIR instruments, respectively.

Atomic force micrographs were obtained by use of a Multimode Nanoscope IIIa SPM (Digital Instruments, St. Barbara, CA) operating in the tapping mode. The measurements were performed at ambient conditions by use of Si cantilevers with a spring constant of ca. 20 N/m and a resonance frequency of about 265 kHz. The set-point amplitude ratio was maintained at 0.9 to minimize the sample deformation from contact with the tip. The samples for AFM measurements were prepared by spin casting of a dilute solution of polymer brushes in DCB on a rotating mica surface at 2000 rpm.

**2-Hydroxyethyl 2'-Bromopropionate.** A 500 mL three-neck round-bottomed flask was charged with 31 g (0.50 mol) of ethylene glycol, 250 mL of anhydrous THF, and 8.0 mL (0.057 mmol) of triethylamine (TEA). The flask was cooled to 0 °C in ice-water, and a solution of 10.8 g (0.050 mol) of 2-bromopropionyl bromide and 100 mL of THF was added dropwise under nitrogen. The mixture was stirred overnight, warming to room temperature of its own accord. Solids were removed by filtration, and the solvent was evaporated. The remaining liquid was redissolved in 200 mL of deionized water and extracted with chloroform. The organic phase was dried over anhydrous  $\text{MgSO}_4$ , and the solvent was removed. The remaining liquid was vacuum-distilled (bp 85–87 °C at 2.1 mmHg) to yield 4.24 g (43%) of colorless liquid HEBP.  $^1\text{H}$  NMR (300 MHz,  $\text{CDCl}_3$ ):  $\delta$  1.92 [3 H,  $\text{CH}(\text{CH}_3)\text{Br}$ ]; 1.99 (1 H,  $\text{HOCH}_2\text{CH}_2\text{O}$ ); 3.91 (2 H,  $\text{HOCH}_2\text{CH}_2\text{O}$ ), 4.28 (2 H,  $\text{HOCH}_2\text{CH}_2\text{O}$ ), 4.33 [1 H,  $\text{CH}(\text{CH}_3)\text{Br}$ ].

**SWNT Initiator.** A 100 mL round-bottomed flask was charged with 50 mg of the carboxylic acid-functionalized SWNT, 50 mL of  $\text{SOCl}_2$ , and 2 mL of DCB. The flask was fitted with a water condenser, and the mixture was stirred at 65 °C for 30 h. The solvent was removed under vacuum. The remaining solid was washed three times with anhydrous THF and was vacuum-dried at 25 °C for 0.5 h. A mixture of the solid, 1.0 g (5.1 mmol) of HEBP, and 50 mL of anhydrous THF was refluxed for 45 h. The solid was separated by filtration through a 0.2  $\mu\text{m}$  poly(tetrafluoroethylene) (PTFE) membrane; thoroughly washed with THF, methanol, and diethyl ether; and vacuum-dried for 10 h to yield 45 mg of the initiator-functionalized SWNT. Anal. Found: C, 92.16; H, 0.31; Br, 2.55, which corresponds to 4.1 initiator groups per 1000 carbons. TGA showed 11.5% weight loss at 500 °C from SWNT-initiator and 4.2% weight loss from the nitric acid-treated SWNT. The difference in weight loss corresponds to 4.3 initiator functions per 1000 carbons of SWNT-initiator.

**Polymer Brushes.** A sealed 50 mL dried Schlenk flask containing SWNT-initiator (15 mg; 0.0048 mmol of initiator groups) and bipy (32.8 mg; 0.210 mmol) was degassed and refilled with nitrogen three times. Deoxygenated nBMA (8.96 g; 63.0 mmol), MBP (16.7 mg; 0.100 mmol) and 5 mL of DCB were added via syringe, and the reaction mixture was degassed by four freeze-pump-thaw cycles. After the mixture was stirred for 1 h at 25 °C, an initial kinetic sample was taken. Then CuCl (10.4 mg; 0.105 mmol) was added, and the flask was placed in a thermostated oil bath at 60 °C. Samples were removed to analyze conversion by  $^1\text{H}$  NMR by comparison with DCB as internal standard and to analyze molecular weight by SEC. The samples for SEC were purified by passing through a column of alumina and a 0.2  $\mu\text{m}$  PTFE filter. After 19 h the polymerization was stopped at 72.5% conversion by cooling to 25 °C and opening the flask to air. The mixture was diluted with 200 mL of DCB, bath-sonicated for 1 h, and filtered through a 0.2  $\mu\text{m}$  PTFE membrane. The solid was washed with DCB to remove the free polymer and  $\text{Cu}^{\text{II}}$ /Bipy complex. After 10 washings there was no cloudiness when 5 drops of colorless filtrate was added to 10 mL of methanol, indicating that little or no soluble PnBMA remained. A pale gray solid was obtained after vacuum-drying for 30 h.

(47) Mansky, P.; Liu, Y.; Huang, E.; Russell, T. P.; Hawker, C. *Science* **1997**, *275*, 1458–1460.

(48) Ito, Y.; Ochiai, Y.; Park, Y. S.; Imanishi, Y. *J. Am. Chem. Soc.* **1997**, *119*, 1619–1623.

(49) Jordan, R.; Ulman, A. *J. Am. Chem. Soc.* **1998**, *120*, 243–247.

(50) Jordan, R.; Ulman, A.; Kang, J. F.; Rafailovich, M. H.; Sokolov, J. *J. Am. Chem. Soc.* **1999**, *121*, 1016–1022.

(51) Weck, M.; Jackiw, J. J.; Rossi, R. R.; Weiss, P. S.; Grubbs, R. H. *J. Am. Chem. Soc.* **1999**, *121*, 4088–4089.

(52) Matyjaszewski, K.; Xia, J. *Chem. Rev.* **2001**, *101*, 2921–2990.

(53) Liu, J.; Rinzler, A. G.; Dai, H.; Hafner, J. H.; Bradley, R. K.; Boul, P. J.; Lu, A.; Iverson, T.; Shelimov, K.; Huffman, C. B.; Rodriguez-Macias, F.; Shon, Y.-S.; Lee, T. R.; Colbert, D. T.; Smalley, R. E. *Science* **1998**, *280*, 1253–1256.

(54) Herrera, J. E.; Resasco, D. E. *Chem. Phys. Lett.* **2003**, *376*, 302–309.

**Cleavage of PnBMA from SWNT.** By the method of Boerner et al.,<sup>42</sup> a 50 mL round-bottomed flask was charged with 20 mg of SWNT-g-PnBMA, 15 mL of DCB, 7 mL of 1-butanol, and 0.5 mL of concentrated sulfuric acid. The flask was fitted with a water condenser, and the mixture was stirred at 95–100 °C for 7 days. The solvent was removed under vacuum, and residual solid was dispersed in chloroform. After an extraction with a small amount of water, the organic phase was isolated and the solvent was distilled off. The remaining solid was dispersed in anhydrous THF, SWNT were removed by filtration through a 0.2  $\mu\text{m}$  PTFE membrane, and the molecular weight of PnBMA in the filtrate was analyzed by SEC.

## Results and Discussion

**Immobilization of ATRP Initiators onto the SWNT.** After treatment with nitric acid to remove residual catalyst, SWNT are functionalized with carboxylic acid groups at the open ends and at defects of the sidewalls.<sup>17,53,55</sup> Scheme 1 shows the methods for ATRP initiator fixation to the carboxylic acid groups and polymerization. The 2-bromopropionate group is an excellent ATRP initiator for living radical polymerization of (meth)acrylate monomers.<sup>52</sup>

The initiator-functionalized SWNT (SWNT-initiator) disperses into organic solvents such as DCB, dimethylformamide (DMF), and chloroform well enough to observe very broad bands in <sup>1</sup>H NMR spectra, but it flocculates as black fiber bundles suspended in clear solvent in less than one week. The IR spectrum shown later has an ester carbonyl band. For these reasons we conclude that the initiators are covalently bound to the SWNT, not just adsorbed. Elemental analysis for Br shows approximately 4.1 initiator functions/1000 carbon atoms. TGA gives about 4.3 initiator functions/1000 carbon atoms. Previous analysis of nitric acid-treated SWNT (Carbon Solution, Inc.) showed 7 carboxylic acid groups/1000 carbon atoms and additional quinone and phenolic groups.<sup>56</sup>

**ATRP of *n*-Butyl Methacrylate from SWNT-Initiator.** The ATRP of *n*-butyl methacrylate (nBMA) was carried out in DCB at 60 °C with CuCl/bipy as catalyst and SWNT-initiator plus soluble methyl 2-bromopropionate (MBP) in a 1/20 mole ratio as initiators. The “halogen exchange” technique of CuCl catalyst with a bromo initiator was used because when the initiator yields a secondary alkyl radical and the monomer is a methacrylate that yields a tertiary radical, it affords better control of the polymerization.<sup>43,57</sup> The free initiator MBP also serves to control the polymerization. Polymerization of methyl methacrylate from an ATRP initiator functionalized on a silicon wafer with no added soluble initiator gave soluble homopolymers with  $M_n$  values independent of monomer conversion and high polydispersities ( $M_w/M_n > 3$ ).<sup>37</sup> The reason for this “uncontrolled” polymerization was that the low concentration of initiator and hence the concentration of Cu<sup>II</sup> complex in the solution was too low to control the polymerization, whereas the polymerization was controlled well by adding free initiator.<sup>37</sup>

The polymerization was stopped after 19 h at 72.5% monomer conversion by <sup>1</sup>H NMR. The conversion of monomer to polymer and evolution of  $M_n$  and  $M_w/M_n$  of the free polymer in the solution are presented in Figure 1. The semilogarithmic kinetic

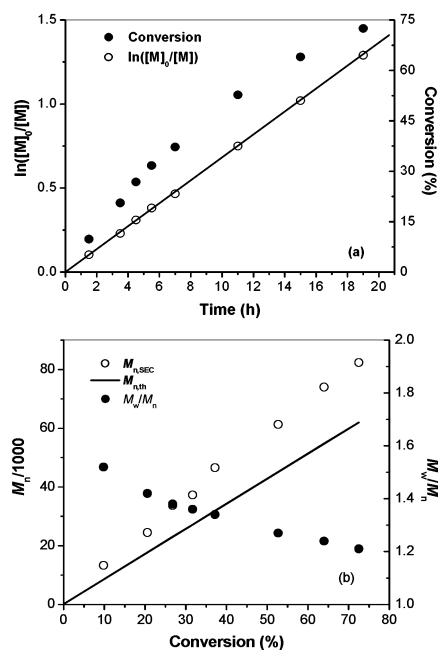


**Figure 1.** Dependence of  $\ln([M]_0/[M])$  and conversion on time (a) and dependence of  $M_n$  and  $M_w/M_n$  on conversion (b) during the brush synthesis. Molecular weight and molecular weight distribution were measured for the linear PnBMA. The line in panel b shows theoretical  $M_n$ . Conditions: [nBMA]:[initiator]:[CuCl]:[Bipy] = 600:1:1:2 in DCB at 60 °C; initiator = SWNT-initiator + MBP with [SWNT-initiator]/[MBP] = 1/20.

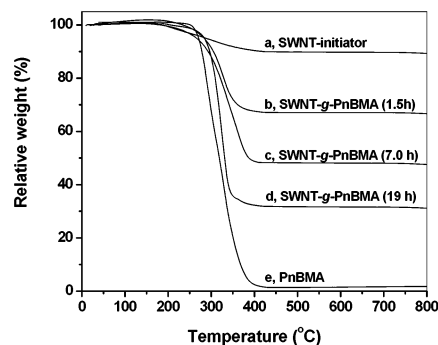


**Figure 2.** TGA thermograms of SWNT-initiator (a), SWNT-g-PnBMA taken at different time intervals (b–d), and PnBMA (e) under nitrogen. The weight left at 500 °C is (a) 88.8%; (b) 66.5%; (c) 47.7%; (d) 31.2%, and (e) less than 1.5%.

plot is linear and passes through the origin, demonstrating that the number of active propagating species in solution is constant throughout the polymerization. The molecular weights measured by SEC increase linearly with monomer conversion, and the polydispersity of the free polymer is low ( $M_w/M_n = 1.21$ ). Therefore the polymerization process is controlled with a negligible contribution of transfer and terminations.

The relative amount of grafted polymer, compared with that of SWNT, was determined by TGA. The pristine HiPco SWNT decompose at 500 °C in air and lose less than 1% of their mass at 800 °C under nitrogen. The nitric acid-treated SWNT lost 4.2% of their mass at 800 °C under nitrogen. Figure 2 shows the TGA traces of SWNT-initiator, SWNT-g-PnBMA, and PnBMA under nitrogen. All of the initiator moieties (Figure 2a) and bulk PnBMA (Figure 2e) are assumed to be lost at 800 °C, leaving residual SWNT. Figure 3 shows that the weight of grafted polymer increases linearly with  $M_n$  of the free polymer. Therefore the number of graft sites on SWNT is almost constant

- (55) Hamon, M. A.; Chen, J.; Hu, H.; Chen, Y.; Itkis, M. E.; Rao, A. M.; Eklund, P. C.; Haddon, R. C. *Adv. Mater.* **1999**, *11*, 834–840.  
 (56) Hu, H.; Bhowmik, P.; Zhao, B.; Hamon, M. A.; Itkis, M. E.; Haddon, R. C. *Chem. Phys. Lett.* **2001**, *345*, 25–28.  
 (57) Shipp, D. A.; Wang, J.-L.; Matyjaszewski, K. *Macromolecules* **1998**, *31*, 8005–8008.

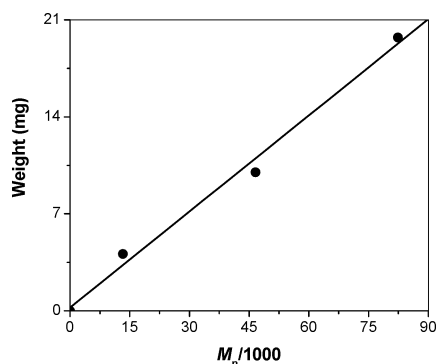


**Figure 3.** Relationship of amount of polymer grafted to 15 mg of SWNT-initiator and  $M_n$  of free polymer produced in solution.

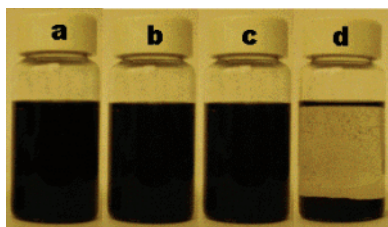


**Figure 4.** Stability in DCB of SWNT-g-PnBMA ( $t = 0$ ) (a), SWNT-g-PnBMA ( $t = 8$  months) (b), nitric acid-treated SWNT ( $t = 0$ ) (c), and nitric acid-treated SWNT ( $t = 10$  min) (d).

during the course of polymerization; i.e., the growth of PnBMA from SWNT is controlled.

Free PnBMA was removed from the SWNT-g-PnBMA by extensive washing with DCB. The grafted PnBMA was cleaved from SWNT by acid-catalyzed transesterification in 1-butanol to ensure that the *n*-butyl ester groups of the PnBMA remained intact during reaction. SEC analysis of the cleaved PnBMA ( $M_n = 8.18 \times 10^4$ ,  $M_w/M_n = 1.25$ ) is similar to that of the free PnBMA produced at the same time ( $M_n = 8.24 \times 10^4$ ,  $M_w/M_n = 1.21$ ), indicating that the growth of PnBMA from SWNT is the same as that of PnBMA initiated with free MBP via ATRP.

The solubility of the SWNT-g-PnBMA depends on the amount of grafted polymer. For example, the sample of the first data point in Figure 3, which contains 22% PnBMA and 78% SWNT-initiator, disperses well in DCB as a black suspension for 2 days before noticeable flocculation but precipitates from chloroform and THF in a few hours. The sample that contains 40% PnBMA and 60% SWNT-initiator forms a solution in DCB indefinitely and flocculates after a few days in chloroform and THF. The highest conversion sample, which contains 57% PnBMA and 43% SWNT-initiator, is stable for weeks as black solutions in DCB, chloroform, and THF. The longest time that we kept a solution of SWNT-g-PnBMA in DCB was 8 months as shown in Figure 4. Without attached polymer the SWNT precipitate in 10 min. Previous attempts to disperse SWNT into solvents with adsorbed polymers have shown polyacrylates and polymethacrylates to be poor dispersants. All of the evidence supports solubilization of the SWNT by covalently bound polymer and not adsorbed polymer.

**Characterization of the SWNT Brushes.** Figure 5 shows the  $^1\text{H}$  NMR spectra of PnBMA (a) and SWNT-g-PnBMA (b) in  $\text{CDCl}_3$ . The spectra are generally similar, both due to PnBMA. The broader signals in the spectrum of PnBMA-g-SWNT may be due to residual paramagnetic materials (iron

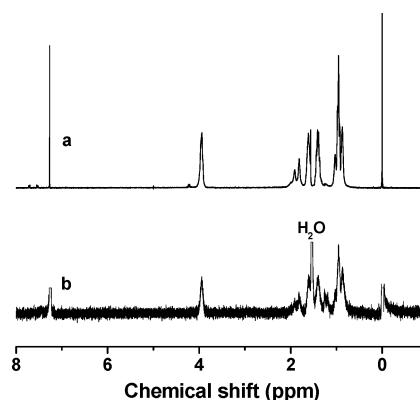


**Figure 5.**  $^1\text{H}$  NMR spectra of PnBMA (a) and SWNT-g-PnBMA (b).

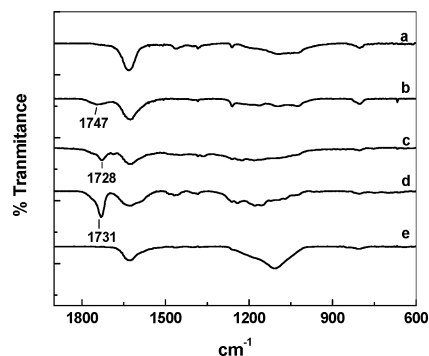


**Figure 6.** Mid-IR spectra of pristine HiPco SWNT (a), nitric acid-treated SWNT (b); SWNT-initiator (c), SWNT-g-PnBMA (d), and SWNT recovered from SWNT-g-PnBMA after TGA (e).

catalyst), local field effects due to SWNT itself, or slow tumbling of the very large polymer brush in solution. NMR line widths alone do not rule out the spectrum coming from soluble polymer.

Figure 6 presents mid-IR spectra. Compared with pristine SWNT (Figure 6a), a new peak around  $1747\text{ cm}^{-1}$  appeared after nitric acid treatment (Figure 6b), which is assigned to non-hydrogen-bonded carboxylic acid groups.<sup>58</sup> The peak shifted to  $1728\text{ cm}^{-1}$  after functionalization with ATRP initiator (Figure 6c), indicating conversion to ester groups. After polymerization, the spectrum (Figure 6d) shows a strong peak at  $1731\text{ cm}^{-1}$  from the ester group of PnBMA. TGA treatment at  $800\text{ }^\circ\text{C}$  removed the PnBMA from the SWNT, and no carbonyl group absorption remained (Figure 6e).

Single molecules of polymer brushes can be visualized by AFM.<sup>59</sup> The pristine HiPco SWNT aggregate into large bundles several micrometers in length and several tens to a hundred nanometers in diameter. It is difficult to observe individual SWNT by AFM without functionalization. Less than a monolayer of SWNT-g-PnBMA brushes was prepared by spin-casting a dilute solution in DCB onto a mica surface and analyzed by tapping mode AFM. Figure 7 shows the conformation of the SWNT-g-PnBMA backbone on a mica surface. The contour lengths range from 200 nm to  $2.0\text{ }\mu\text{m}$ , and the average height of the backbone is about 2–3 nm. The diameters of individual HiPco SWNT range from 0.6 to 1.3 nm.<sup>60</sup> Since the PnBMA

(58) Zhang, J.; Zou, H. L.; Qing, Q.; Yang, Y. L.; Li, Q. W.; Liu, Z. F.; Guo, X. Y.; Du, Z. L. *J. Phys. Chem. B* **2003**, *107*, 3712–3718.

(59) Sheiko, S. S.; Prokhorova, S. A.; Beers, K. L.; Matyjaszewski, K.; Potemkin, I. I.; Khokhlov, A. R.; Moeller, M. *Macromolecules* **2001**, *34*, 8354–8360.

(60) Bachilo, S. M.; Strano, M. S.; Kittrell, C.; Hauge, R. H.; Smalley, R. E.; Weisman, R. B. *Science* **2002**, *298*, 2361–2366.

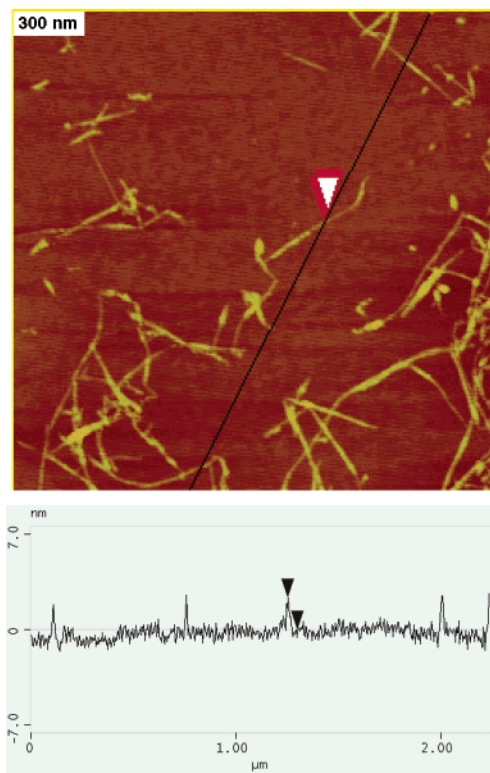


**Figure 7.** AFM height image and section analysis of SWNT-g-PnBMA brushes. The arrows point to a 2.3 nm height difference.

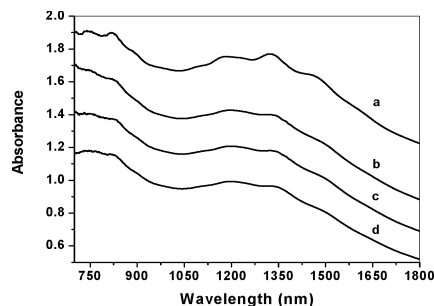


**Figure 8.** NIR spectra of pristine HiPco SWNT (a), nitric acid-treated SWNT (b), SWNT-initiator (c), and SWNT-g-PnBMA (d).

side chains thicken the backbone in AFM images, the 2–3 nm height is consistent with single tubes, although aggregates of 2–3 SWNT could also be responsible for the AFM results.

**Near-IR and Raman Spectra.** One major advantage of this polymer functionalization method is retention of the electronic and thermal properties of the nitric acid-treated SWNT. Raman and near-IR spectroscopy provide qualitative information about the electronic state of the SWNT-g-PnBMA. As shown in Figure 8a, the near-IR absorption spectrum of pristine HiPco SWNT contains peaks due to the van Hove singularities, which are the band gap transitions in semiconducting nanotubes from about 1400 to 800 nm. The band frequencies depend on the tube diameter and chirality.<sup>60</sup> If the nanotubes are significantly modified by covalent sidewall functionalization, creating a much larger number of compounds, these bands recede and a smooth curve appears in the near-IR spectra.<sup>25</sup> Figure 8b–d shows the near-IR spectra of the nitric acid-treated tubes, the SWNT-initiator, and the SWNT-g-PnBMA, respectively. Compared with that of pristine SWNT (spectrum a), the intensity of the

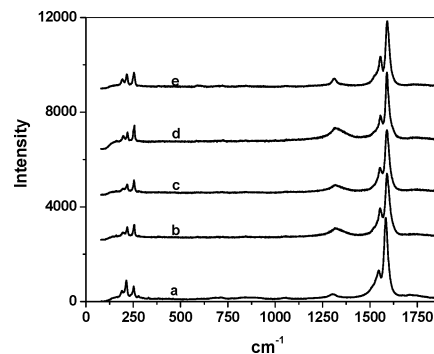


**Figure 9.** Raman spectra of pristine HiPco SWNT (a), nitric acid-treated SWNT (b), SWNT-initiator (c), SWNT-g-PnBMA (d), and SWNT recovered from SWNT-g-PnBMA after TGA (e).

peaks at 1400–800 nm in spectra b–d is weaker but still present. Furthermore, there is no significant change in curves c and d compared with that of curve b. The results indicate that the nitric acid treatment produced defects on sidewalls of the SWNT and that transformation of the nitric acid-treated SWNT to the SWNT-initiator and grafting PnBMA did not change further the electronic structure of the SWNT.

Raman spectra also indicate the status of sidewall functionalization. Figure 9a is the Raman spectrum from excitation at 633 nm of pristine HiPco SWNT, in which the signals around 180–260 and 1590  $\text{cm}^{-1}$  are the diameter-dependent radial breathing ( $\omega_r$ ) mode and the tangential ( $\omega_t$ ) mode, respectively. A third mode, the so-called disorder mode or  $\text{sp}^3$  mode, appears around 1295  $\text{cm}^{-1}$  if the sidewalls of the SWNT are functionalized by covalent attachment. The Raman spectra in Figure 9b–e show that the nitric acid treatment caused a small increase in the  $\text{sp}^3$  mode signal compared with that of the pristine SWNT (Figure 9a) and that subsequent functionalization to SWNT-initiator and graft PnBMA did not increase the intensity of the  $\text{sp}^3$  mode in their Raman spectra. Furthermore, the intensity of  $\text{sp}^3$  mode signal decreased (Figure 9e) after heating to 800 °C under nitrogen, which indicates that the structure of the original SWNT was substantially recovered by defunctionalization. Similar defunctionalization has been reported before.<sup>25</sup>

## Conclusions

ATRP of nBMA from SWNT is controlled well by adding free initiator in the reaction system. The amount of PnBMA grafted to SWNT increases linearly with the molecular weight of the free PnBMA. AFM shows that the functionalized SWNT spreads well on mica surface and that the bundles of nitric acid-treated HiPco SWNT were broken into individual tubes by functionalization and polymerization. Mid-IR, near-IR, and Raman spectra show that nitric acid oxidation creates carboxylic acid groups on the SWNT and that the further conversion to grafted PnBMA has no significant effect on the structure of the underlying SWNT.

The formation of polymer brushes from SWNT should be applicable to any polymer that can be grafted from an initiator bound to SWNT. The ATRP method should enable grafting of a wide range of vinyl polymers. Blending of the SWNT brushes into the parent polymers will increase their tensile strength and their electrical and thermal conductivity.<sup>6,8</sup> By comparison, the noncovalent adsorption of polymer or surfactant to SWNT is limited to fewer polymers and surfactants, and in some cases

the adsorbed materials are reported to be stable only for limited time. Individual SWNT revert to bundles if the free surfactant is removed.<sup>61</sup> The SWNT-g-PnBMA are stable for at least 8 months in DCB solution. With ATRP, the chain length of polymer grown from SWNT is adjustable by control of the

(61) Richard, C.; Balavoine, F.; Schultz, P.; Ebbesen Thomas, W.; Mioskowski, C. *Science* **2003**, *300*, 775–778.

monomer/initiator ratio or the monomer conversion, and block copolymers might also be grown from SWNT.

**Acknowledgment.** Financial support from the National Science Foundation (EPS-0132543) is gratefully acknowledged. We thank LeGrande Slaughter for use of the TGA.

JA037937V